ACS Macro Letters

Letter

pubs.acs.org/macroletters

Kinetic Pathway of the Cylinder-to-Sphere Transition in Block Copolymer Micelles Observed in Situ by Time-Resolved Neutron and Synchrotron Scattering

Reidar Lund,*[,†] Lutz Willner,[‡] Dieter Richter,[‡] Peter Lindner,[§] and Theyencheri Narayanan[∥]

[†]Department of Chemistry, University of Oslo, Postboks 1033 Blindern, 0315 Oslo, Norway

[‡]Jülich Centre for Neutron Science JCNS and Institute for Complex Systems ICS, Forschungszentrum Jülich GmbH, 52425 Jülich, Germany

[§]Institut Laue-Langevin (ILL), F-38042 Grenoble, France

[∥]European Synchrotron Radiation Facility (ESRF), F-38043 Grenoble, France

Supporting Information

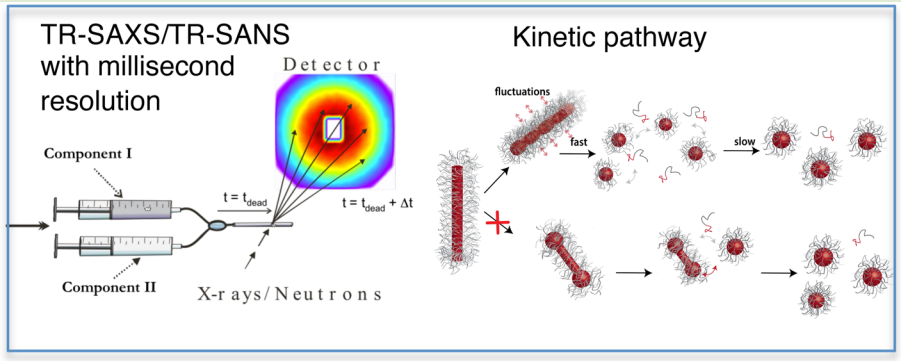

ABSTRACT: Here we present an in situ study of the nonequilibrium cylinder-to-sphere morphological transition kinetics on the millisecond range in a model block copolymer micelle system revealing the underlying mechanism and pathways of the process. By employing the stopped-flow mixing technique, the system was rapidly brought (≈100 μs) deep into the instability region, and the kinetics was followed on the time scale of milliseconds using both time-resolved small-angle neutron and X-ray scattering (TR-SANS and TR-SAXS, respectively). Due to the difference in contrast and resolution, SAXS and SANS provide unique complementary information. Our analysis shows that the morphological transition is characterized by a single rate constant indicating a two-state model where the transition proceeds through direct decomposition (fragmentation) of the cylinders without any transient intermediate structures. The cylindrical segments formed in the disintegration process subsequently grow into spherical micelles possibly through the molecular exchange mechanism until near equilibrium micelles are formed. The observation of a two-step kinetic mechanism, fluctuation-induced fragmentation and "ripening" processes, provides unique insight into the nonequilibrium behavior of block copolymer micelles in dilute solutions.

Block copolymers are polymorphic systems which form a wide range of structures such as spheres, cylinders, and vesicles in selective solvents, i.e., solvents which are good for one block and poor for the other.[1,2] The factors determining the structural properties relate to a range of molecular parameters such as chemical compositions of monomers, molecular weight, and block composition,[3−5] as well as temperature[6,7] and solvent quality.[8−10] In general, the self-assembly process of block copolymers yields a reasonably predictable micellar entity if the system is able to attain equilibrium, i.e., it is *thermodynamically controlled*. However, it has become increasingly clear over the last years that many block copolymer systems are nonergodic which may lead to nonequilibrium structures that depend on the method of preparation.[11] These structures are *kinetically controlled*.[12−14] This can be attributed to slow equilibrium kinetics associated with high activation barriers, where relaxation pathways such as molecular (chain) exchange kinetics are many orders of magnitude slower than in surfactant systems[15−21] and fusion/fission pathways are strongly suppressed due to osmotic repulsion between micellar entities with extended coronas.[15] In light of the slow equilibration pathways of block copolymer micelles, it is of interest to consider the transition kinetics from one morphological state to another and ask the following questions: by which mechanism does the transition proceed and are any intermediate nonequilibrium structures involved? The latter question is particularly

Received: October 9, 2013
Accepted: November 25, 2013
Published: November 26, 2013

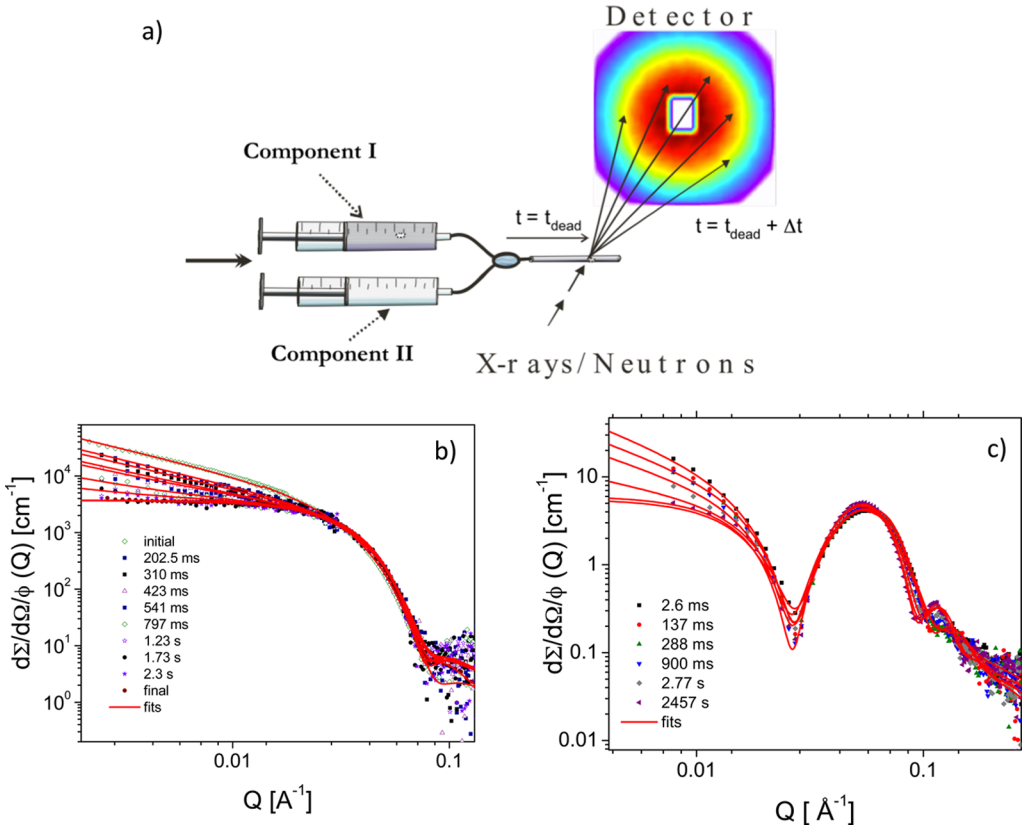

Figure 1. (a) Experimental setup using a stopped-flow apparatus is coupled with a SAXS and SANS instrument allowing an in situ observation of the morphological transition. Time-resolved neutron and X-ray scattering data showing the transition from cylindrical to spherical micelles in real time are depicted in (b) and (c), respectively. The data are obtained after mixing 1.5 vol % PEP1−PEO1 in 51% dDMF/D_2O solution with pure dDMF 1:1 in a stopped-flow apparatus. The data in (b) are obtained from SANS at D11, ILL (Grenoble), while (c) represents selected SAXS data from ID02, ESRF (Grenoble). The time resolution is set by the deadtime and acquisition time that was 2.3 ms/5 ms and 50 ms/200 ms for SAXS and SANS, respectively.

interesting for potential strategies where "frozen in" nonequilibrium micelles are used to yield well-defined nanostructures. Hence, by understanding the kinetics, predictive schemes to design and produce well-defined nanoparticles with predefined dynamic and structural properties can be developed.

A deeper understanding of the nonequilibrium kinetics of self-assembling polymer systems necessitates direct experimental observations which are very challenging due to rapid kinetics (typically down to the millisecond range) and limited experimental structural resolution. Consequently, kinetic studies of morphological transitions in block copolymer micellar systems are rare and are mostly related to ordering kinetics and morphological transition in melts or concentrated solutions. Examples include disorder to order,[22] lamella-to-cylinder,[23] cylinder-to-sphere,[24] and cylinder-to-gyroid[25] transition kinetics. Eisenberg et al. explored the kinetics and mechanisms of various transitions of polystyrene−poly(acrylic acid) (PS−PAA) block copolymers in water/1,4-dioxane mixtures.[8] In a paper by Burke and Eisenberg[26] using TEM and turbidity measurements they found that the cylinder to sphere transition starts with the formation of bulbs at the end of the rods which in the rate-determining second step are released from the ends of the cylindrical body. This contrasts conclusions from earlier work for block copolymer melts undergoing a cylinder-to-sphere morphological transition.[27−31] Here the spherical bcc phase is believed to grow epitaxially along the cylinder axis facilitated by strong undulations.[28] To summarize, there are two possible kinetic pathways potentially present in block copolymer solutions which we may refer to as: (i) fluctuation-induced direct decomposition (FIDD) mechanism and (ii) a sphero-cylinder mediated (SCM) transition mechanism. To investigate and distinguish these mechanisms, it is necessary to study the process in situ using experimental methods capable of providing nanoscale resolution on suitable times scales starting from milliseconds.

In this letter we specifically address the nature of the kinetic pathway of the cylinder to sphere transition aiming to determine whether the transition proceeds through transient intermediates. By employing modern time-resolved small-angle neutron and X-ray scattering (TR-SANS and TR-SAXS, respectively) techniques, we are able to directly probe the nanostructural evolution in situ on times scales starting from only a few milliseconds using a strategy previously used for surfactant micelles.[32−38] Synchrotron TR-SAXS techniques combined with a stopped-flow apparatus designed for rapid mixing have recently also been used to study the micellization kinetics of both regular (low molecular weight) surfactant[39] and block copolymer[40] micelles. Here we explore the complementarity between SAXS and SANS to provide unique insight into the morphological transition. The results suggest a direct decomposition of the cylinders into spherical micelles, i.e., a fluctuation-induced direct decomposition (FIDD) mechanism followed by a ripening process where the spherical micelles

dx.doi.org/10.1021/mz400521p | ACS Macro Lett. 2013, 2, 1082−1087

grow in time in an independent fashion until a stationary (near equilibrium) state is reached.

In this study, we employ a model system consisting of poly(ethylene-*alt*-propylene)−poly(ethylene oxide) (PEP1−PEO1, the numbers indicate approximate molecular weight in kg/mol) block copolymer solutions in D_2O (Armar AG Switzerland 99.8% D) and DMF-d_7 ("dDMF", Chemotrade, Leipzig 99.5% D) mixtures. The system has been studied previously[10,41] where it was found that in water-rich solution cylindrical micelles are formed due to the high entropic penalty associated with the chain stretching in the core at high interfacial tensions. However, above 50% dDMF/D_2O the morphology changes from cylindrical to spherical micelles.[10]

Figure 1 shows the experimental setup and data obtained in a stopped-flow experiment (Biologic, SFM 400) using both time-resolved SAXS (ID02/ESRF) and SANS (D11/ILL) available at the European Photon and Neutron Campus (EPN) in Grenoble, France. The experiments, performed using the same samples, are initiated after rapid 1:1 mixing of a 1.5 vol % micellar 51 mol % D_2O/dDMF solution with pure dDMF which brings the system almost "instantaneously" (≈100 μs) deep into the instability region where spherical micelles are preferred over cylindrical ones.

The normalized SANS and SAXS intensity data plotted as a function of the modulus of the momentum transfer vector Q ($Q = 4\pi \sin(\theta/2)/\lambda$, where λ and θ are the wavelength and scattering angle, respectively) are given in Figures 1(b) and (c). Comparing the data we see that the shape of the data is completely different. This is a consequence of the very different scattering contrast for X-rays and neutrons. While for neutrons the contrasts to both blocks are large and negative, the scattering contrast for X-ray is of opposite magnitude for the two blocks such that the system is almost contrast matched on average. Consequently, SANS is sensitive to the overall morphological change, while SAXS renders the internal structure of the micelle visible, with only a hint of information about the morphology at the lowest Q.

Considering the SANS data first, it is evident that the scattering pattern changes considerably, in particular at the lowest Q where the intensity decays significantly. Moreover, the data demonstrate a change in slope at low Q where a Q^{-1} behavior is visible at short times, whereas a plateau-like (Guinier-like) scattering is observed at longer times clearly demonstrating a morphological transition from cylinders to spheres. Initially the SANS data were fitted using several theoretical scattering models. At first, several core−shell scattering models were considered, including regular cylinders or sphero-cylinders of variable lengths in coexistence with spherical micelles. However, it turned out that the data could be fitted rather satisfactorily using a simple model describing a linear combination of spherical and cylindrical micelles. It is particularly interesting to note that attempts using more "detailed" scattering models for cylinders with spherical end-caps ("sphero-cylinders/dumbbells")[42] did not improve the fit quality.

Consequently the data were modeled using a simple coexistence of spherical and cylindrical core−shell particles

$$I(Q,t)/\phi = f_{cyl}(t)I(Q,t)_{cyl} + (1 - f_{cyl}(t))I(Q,t)_{sphere} \quad (1)$$

where f_{cyl} is the fraction of cylindrical micelles in the solution and the $I(Q,t)_{sphere}/I(Q,t)_{cyl}$ represent the scattered intensity calculated from core−shell models for cylinders and spheres using expressions reported in detail in ref 10 and described in the Supporting Information.

The TR-SAXS data in Figure 1(b) also show a time dependence, but as expected from the contrast situation, the evolution is much more subtle. However, the SAXS data show a much better resolution at higher Q such that the internal structure of the micelles can be analyzed in detail. To get the maximum insight into the kinetic mechanism and the structural evolution, we therefore proceeded to seek a simultaneous description of the complementary sets of data using the same scattering model. For consistency, a refinement approach was applied where the fit parameters from each data set were used to describe the other in an iterative fashion. First this model was fitted to the SANS data by fixing the micellar parameters of the cylindrical and spherical micelles corresponding to the "initial" and "final" states, respectively, allowing only f_{cyl} to vary. Using this initial approximation the SANS data could be rather well described. However, the fit quality of the SAXS data was comparably poor which was particularly reflected in a failure to describe the shift in the maximum/minimum with time visible in Figure 1(c). To improve the fit quality, the parameters corresponding to the spherical micelles were set free (aggregation number, P, thickness of micellar corona, $D = R_m - R_c$ where R_c and R_m are the core and overall micellar radius, respectively). The fraction, f_{cyl}, was fixed to the values found from SANS by parametrizing the time dependence. The procedure was then repeated until a good agreement was reached.

The result showing the time dependence of f_{cyl} as deduced by SANS is displayed in Figure 2(a). As indicated by the solid line, the data are rather perfectly described by a single exponential decay: $f_{cyl} = \exp(-t/\tau)$. Equivalently, this is indicated with a straight line in a semilogarithmic plot. From the fits we determined the characteristic relaxation time of $\tau = 328 \pm 20$ ms. The simple time dependence and the single rate constant are other good indications that transformation from cylinders

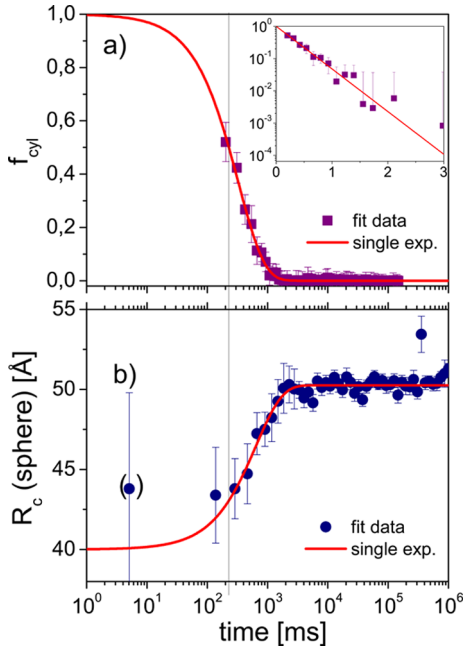

Figure 2. Time dependence of (a) the fraction f_{cyl} and (b) the core radius of the spherical micelles deduced from the fits of the scattering data using eq 1.

dx.doi.org/10.1021/mz400521p | *ACS Macro Lett.* 2013, 2, 1082−1087

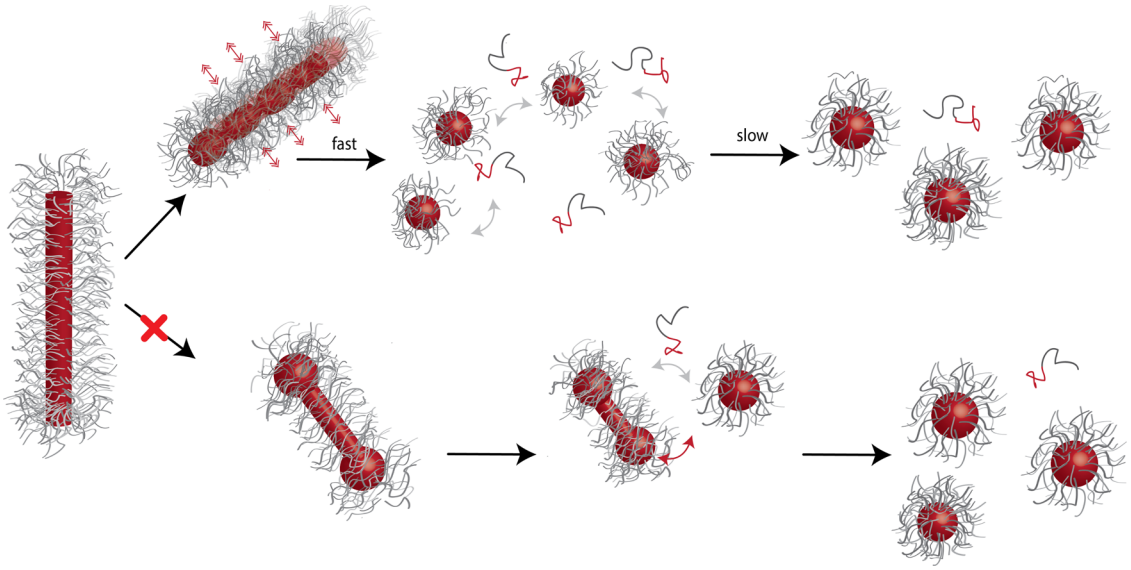

Figure 3. Schematic illustration of two possible mechanisms for the cylinder-to-sphere transition in block copolymer micelles: in the upper part, the direct fluctuation-induced decomposition (FIDD) mechanism suggested in this work is depicted. Here the large instabilities after crossing the phase boundary are expected to tear the cylinders into globular micelles with a single rate constant. The premature, small micelles are thereby seen to "ripen" in time and increase their size via the molecular exchange mechanism (indicated by gray arrows). The lower part displays the transition proceeding via the formation of dumbbell-like micelles as intermediates—the sphero-cylinder-mediated (SCM) transition mechanism. The decomposition proceeds via unstable ends of the sphero-cylinder which are released as spherical micelles. See text for more details.

proceeds directly to spheres without any intermediate structures in agreement with the qualitative discussion of the scattering data above.

Interestingly from the fit analysis, an apparent shift of the form factor maximum and minimum toward lower Q in Figure 1(c) can be mainly attributed to an increase in the radius of the spherical micelle, R_c, with time. This feature is not observed in the SANS data due to limited resolution. As indicated by the solid lines in Figure 2(b), the time dependence of the core size of the spherical micelles can be described surprisingly well with a simple exponential growth: $R_c(t) = R_c(0) + \Delta R_c(1 - \exp(-t/\tau_c))$ with $\tau_c = 645 \pm 100$ ms and $\Delta R_c = 10 \pm 2$ Å. The initial radius of the spherical micelles extracted from the fits, $R_c(0)$, was found to be close to 40 Å which is close to the radius of the initial cylinders (≈39 Å). Hence, we observe a growth of the spherical micelles starting from, probably, fragments of the original cylinders. This growth process, somehow slower than the decomposition of the cylinders, can be attributed to a growth process similar to Ostwald ripening that occurs until the micelles reach a size and a size distribution both approaching their close to equilibrium values. However this growth is rather different from a traditional Ostwald ripening process which approximately scales with time as $R_c(t) \sim t^{1/3}$.[43] Instead the process proceeds through a near exponential growth.

The second "ripening" process is likely to reflect micellar exchange which would equilibrate the spherical micelles through a continuous series of unitary step growth events. Indeed, in a previous work, it was found that unimer exchange is the dominant mechanism for equilibrium kinetics in this system[41] and was found to be operational and rather fast for this particular DMF/water solution. However, in light of the rather dramatic effect of polymer chain-length polydispersity[19,44,45] on the chain exchange kinetics, also in this system,[41] it is reasonable to assume a broader relaxation pattern possibly reflected in a stretched exponential growth, i.e., $\sim 1 - \exp(-(t/\tau)^{\beta})$, where $0 < \beta \leq 1$. However, within the experimental errors, no indication of $\beta < 1$ was found. It is interesting to note that the Aniansson–Wall theory[46] would predict a two-step process during the equilibration process. However this theory is only valid very close to equilibrium which is definitely not the case here. Nevertheless, it might be that a second extremely slow mode would occur if this re-equilibration process after spherical micelles were formed would be followed over very long times scales. However as shown in a recent work by Melt et al.,[47] such re-equilibration kinetics might be more complex and even be described with compressed exponentials ($\beta \approx 2$). Alternatively, the exponential growth might reflect another mechanism such as micellar fusion.[48] However, this mechanism is likely to give a very broad distribution of micellar sizes and larger clusters which, rather than a single relaxation time, also would be expected to give a broader relaxation pattern.

It should be mentioned that an alternative explanation would be a decomposition of the cylinders that proceed through the formation of sphero-cylinders which gradually decrease in length.[26,49] In this scenario, the end-caps would grow in size until they become unstable due to the high surface energy associated with the curvature at the junction zone and pinch off as spherical micelles. However, this scenario is not consistent with the SANS data as growing spherical end-caps and decreasing cylinder length would give an excess scattering at intermediate low Q (see Supporting Information). Such a change in shape is not observed. In trial fits the data were analyzed with a coexisting model of sphero-cylinders and spheres. The analysis shows that in all cases the data were best described using (near constant) long cylinder lengths which effectively dilute the contribution of spherical end-groups, thus suggesting that sphero-cylinders are not dominant during the kinetic process.

Hence the combination of SAXS and SANS data with theoretical modeling suggests that the transformation from cylinders proceeds through a fast fragmentation of the cylinders rather than a gradual decrease in cylinder length. The latter is

dx.doi.org/10.1021/mz400521p | ACS Macro Lett. 2013, 2, 1082−1087

also excluded by theoretical modeling where the form factor of a gradually decreasing cylinder length would look different, rather than a decreasing slope of the low Q data in Figure 1(a). One would also expect a reduction in the Q^{-1} region in that case (see Supporting Information). A similar observation was made by TEM where the cylinders seem to undergo direct fragmentation upon changes in pH in a pH-responsive charged system.[50] Similar ideas have also been suggested earlier for block copolymer melts undergoing a cylinder-to-sphere morphological transition.[27,29] Here the spherical bcc phase is believed to grow epitaxially from the cylinder axis which undergoes strong undulations near the critical point. Similar fluctuations can be expected to be present here when the cylindrical micelles are abruptly taken from their region of stability through rapid mixing. As the rapid change in solvent composition from 50 to 75% induces a significant jump in the interfacial tension (from about 15 to 10 mN/m),[51] a strong enhancement of fluctuations is to be expected. This anisotropic fluctuation involves alternating pinching and bulging of the cylindrical domains and probably leads to fragmentation of the cylinders into sphero-like micelles. As these micelles originate from fragments of cylindrical micelles where the cross-sectional radius is naturally smaller than for spherical micelles, a growth is favored by the interfacial energy until unfavorable chain stretching in the core limits further growth and the system approaches equilibrium as described above. The scenario emerging from these results is depicted in Figure 3 and compared to the sphero-cylinder mechanism.

It should be pointed out that the results in this work point toward a different scenario than for "crew-cut" PS−PAA micelles reported by Burke and Eisenberg[26] where the formation of spherical micelles proceeds via sphero-cylinders (SCM mechanism). It is likely that the difference is related to rather small solvent jump amplitudes close to the mesophase boundaries in their work. In the present work rather large jumps (from 50 to 75 mol %) deep into the nonequilibrium region are produced which probably lead to pronounced instabilities and consequently strong fluctuations.

In conclusion, by exploiting the different scattering contrast for X-rays and neutrons in the system, very detailed structural aspects of the micellar transition and evolution have been extracted. The results point toward a direct transition mechanism where the cylinders fluctuate strongly and decompose into spherical micelles. The premature spherical micelles subsequently ripen and grow into the final equilibrium-like micelles. This observation provides experimental support for a fluctuation-induced direct decomposition (FIDD) mechanism present in block copolymer micelles. This mechanism has been proposed, although not directly observed, for both low-molecular-weight surfactant[52] and bulk block copolymer systems.[27,29] A similar mechanism has also been qualitatively suggested based on TEM imaging of a pH-responsive block copolymer solution where undulations were thought to precede a sequence of branching and budding sequences after the cylinders were brought into the instability regime.[50] In this work we provide quantitative evidence of this mechanism and also demonstrate a subsequent "ripening-type" mechanism that has not been observed in earlier works. This two-step kinetic pathway could only be revealed thanks to the combination of high-resolution X-ray data with the neutron data results. Apart from giving almost molecular-level insight into the kinetic pathways for morphological transitions, the results in this work give a very detailed picture of the equilibration mechanism and stability of block copolymer systems. This may prove useful to devise new predictive schemes to design and produce well-defined nanoparticles with predefined dynamic and structural properties. The study also presents an efficient methodology, utilizing the complementarity of X-rays and neutrons, to investigate fast kinetics with nanostructural resolution with great detail.

EXPERIMENTAL SECTION

The h-PEP1−h-PEO1 (hh) polymer is identical with the one used in the structural and kinetic studies published previously.[10,41] It was prepared following the synthetic methods described in ref 53. The block copolymer consists of a PEP block of 1200 g/mol (polydispersity index, PDI = M_w/M_n = 1.06) and a PEO block of 1500 g/mol with overall PDI of 1.04. The samples were prepared by directly dissolving the powder in a 51 mol % dDMF/D_2O solvent mixture. For more info see the Supporting Information. For rapid mixing, a modified commercial stopped-flow apparatus (Biologic, SFM 400) was employed. The reservoirs were mixed by injection into the mixing chamber and transported into the scattering volume using a 2 mL/s mixing speed for each syringe. It was explicitly verified that mixing 51 mol % of DMF with pure DMF does not lead to any measurable increase in the temperature during mixing, and the kinetic process was therefore investigated under isothermal conditions. A special observation cell was set up using a quartz cell (Hellma, 1 mm optical length) for SANS and a quartz capillary (diameter of 1.5 mm/wall thickness of 0.01 mm, Glass Technic) for SAXS. The SANS measurements were carried out using the D11 instrument at Institut Laue Langevin (ILL) in Grenoble, France. The measurements were performed at 6 Å wavelength, several sample-to-detector distances, and collimation lengths to cover an extended Q range and to maintain a reasonable resolution. This mixing and transport takes 50 ms (t_{dead}) and fills the cell, and subsequent measurements were made using 200 ms acquisition time. To improve the statistics, the samples were mixed and measured five times, and the resulting data were combined. Details concerning the calibration/data reduction procedure are given in ref 54. The SAXS measurements were performed at the ID02 High Brilliance beamline at the European Synchrotron Radiation Facility (ESRF) in Grenoble, France, using 12.4 keV photons (corresponding to λ = 1 Å). The acquisition time was 5 ms for each frame with a minimal readout pause of 140 ms between two acquisitions. The recorded kinetic time frames were spaced in a geometric progression to avoid overexposing the sample and possibly induce radiation damage. See the Supporting Information for details.

ASSOCIATED CONTENT

Supporting Information

Additional experimental details: scattering experiments and SAXS/SANS data modeling. This material is available free of charge via the Internet at http://pubs.acs.org.

AUTHOR INFORMATION

Corresponding Author

*E-mail: reidar.lund@kjemi.uio.no.

Notes

The authors declare no competing financial interest.

ACKNOWLEDGMENTS

The authors acknowledge ESRF and ILL for beamtime. Assistance by Dr. Isabelle Grillo and Dr. Jeremie Gummel during the experiments at ILL and ESRF, respectively, is gratefully acknowledged. The authors are also indebted to Dr. Vitaliy Pipich for fruitful discussions. R.L. acknowledges a grant from the Norwegian Research Council, SYNKNOYT, for the project with the number 8411/F50.

REFERENCES

(1) Hamley, I. W. *The Physics of Block Copolymers*; Oxford University Press Inc.: New York, 1998.
(2) Mai, Y.; Eisenberg, A. *Chem. Soc. Rev.* **2012**, *41*, 5969−5985.
(3) Antonietti, M.; Forster, S. *Adv. Mater.* **2003**, *15*, 1323−1333.
(4) Won, Y.-Y.; Brannan, A. K.; Davis, H. T.; Bates, F. S. *J. Phys. Chem. B* **2002**, *106*, 3354−3364.
(5) Kaya, H.; Willner, L.; Allgaier, J.; Stellbrink, J.; Richter, D. *Appl. Phys. A: Mater. Sci. Process.* **2002**, *74*, s499−s501.
(6) Bhargava, P.; Tu, Y.; Zheng, J. X.; Xiong, H.; Quirk, R. P.; Cheng, S. Z. D. *J. Am. Chem. Soc.* **2007**, *129*, 1113−1121.
(7) Wang, L.; Yu, X.; Yang, S.; Zheng, J. X.; Van Horn, R. M.; Zhang, W.-B.; Xu, J.; Cheng, S. Z. D. *Macromolecules* **2012**, *45*, 3634−3638.
(8) Shen, H.; Eisenberg, A. *J. Phys. Chem. B* **1999**, *103*, 9473−9487.
(9) Abbas, S.; Li, Z.; Hassan, P. A.; Lodge, T. P. *Macromolecules* **2007**, *40*, 4048−4052.
(10) Lund, R.; Pipich, V.; Willner, L.; Radulescu, A.; Colmenero, J.; Richter, D. *Soft Matter* **2011**, *7*, 1491.
(11) Jain, S.; Bates, F. S. *Macromolecules* **2004**, *37*, 1511−1523.
(12) Zhang, L.; Eisenberg, A. *Macromolecules* **1999**, *32*, 2239−2249.
(13) Cui, H.; Chen, Z.; Zhong, S.; Wooley, K. L.; Pochan, D. J. *Science* **2007**, *317*, 647−650.
(14) Hayward, R. C.; Pochan, D. J. *Macromolecules* **2010**, *43*, 3577−3584.
(15) Halperin, A.; Alexander, S. *Macromolecules* **1989**, *22*, 2403−2412.
(16) Willner, L.; Poppe, A.; Allgaier, J. *Europhys. Lett.* **2001**, *55*, 667−673.
(17) Lund, R.; Willner, L.; Stellbrink, J.; Lindner, P.; Richter, D. *Phys. Rev. Lett.* **2006**, *96*, 068302.
(18) Lund, R.; Willner, L.; Richter, D.; Dormidontova, E. E. *Macromolecules* **2006**, *39*, 4566−4575.
(19) Choi, S. H.; Lodge, T. P.; Bates, F. S. *Phys. Rev. Lett.* **2010**, *104*, 47802.
(20) Zinn, T.; Willner, L.; Lund, R.; Pipich, V.; Richter, D. *Soft Matter* **2012**, *8*, 623−626.
(21) Lund, R.; Willner, L.; Richter, D. *Kinetics of Block Copolymer Micelles Studied by Small-Angle Scattering Methods*; Springer Berlin Heidelberg: Berlin, Heidelberg, 2013.
(22) Nie, H.; Bansil, R.; Ludwig, K.; Steinhart, M.; Konak, C.; Bang, J. *Macromolecules* **2003**, *36*, 8097−8106.
(23) Jeong, U.; Lee, H. H.; Yang, H.; Kim, J. K.; Okamoto, S.; Aida, S.; Sakurai, S. *Macromolecules* **2003**, *36*, 1685−1693.
(24) Krishnamoorti, R.; Modi, M. A.; Tse, M. F.; Wang, H. C. *Macromolecules* **2000**, *33*, 3810−3817.
(25) Wang, C.-Y.; Lodge, T. P. *Macromolecules* **2002**, *35*, 6997−7006.
(26) Burke, S. E.; Eisenberg, A. *Langmuir* **2001**, *17*, 6705−6714.
(27) Sakurai, S.; Kawada, H.; Hashimoto, T.; Fetters, L. J. *Macromolecules* **1993**, *26*, 5796−5802.
(28) Koppi, K. A.; Tirrell, M.; Bates, F. S.; Almdal, K.; Mortensen, K. *J. Rheol.* **1994**, *38*, 999.
(29) Ryu, C. Y.; Lodge, T. P. *Macromolecules* **1999**, *32*, 7190−7201.
(30) Bendejacq, D.; Joanicot, M.; Ponsinet, V. *Eur. Phys. J. E* **2005**, *17*, 83−92.
(31) Grason, G. M.; Santangelo, C. D. *Eur. Phys. J. E* **2006**, *20*, 335−346.
(32) Egelhaaf, S. U. *Curr. Opin. Colloid Interface Sci.* **1998**, *3*, 608−613.
(33) Gradzielski, M. *Curr. Opin. Colloid Interface Sci.* **2003**, *8*, 337−345.
(34) Gradzielski, M.; Grillo, I.; Narayanan, T. *Prog. Colloid Polym. Sci.* **2004**, *129*, 32−39.
(35) Schmölzer, S.; Gräbner, D.; Gradzielski, M.; Narayanan, T. *Phys. Rev. Lett.* **2002**, *88*, 258301.
(36) Weiss, T.; Narayanan, T.; Wolf, C.; Gradzielski, M.; Panine, P.; Finet, S.; Helsby, W. *Phys. Rev. Lett.* **2005**, *94*, 1−4.
(37) Gummel, J.; Sztucki, M.; Narayanan, T.; Gradzielski, M. *Soft Matter* **2011**, *7*, 5731.
(38) Bressel, K.; Muthig, M.; Prévost, S.; Gummel, J.; Narayanan, T.; Gradzielski, M. *ACS Nano* **2012**, *6*, 5858−5865.
(39) Jensen, G. V.; Lund, R.; Gummel, J.; Monkenbusch, M.; Narayanan, T.; Pedersen, J. S. *J. Am. Chem. Soc.* **2013**, *135*, 7214−7222.
(40) Lund, R.; Willner, L.; Monkenbusch, M.; Panine, P.; Narayanan, T.; Colmenero, J.; Richter, D. *Phys. Rev. Lett.* **2009**, *102*, 188301.
(41) Lund, R.; Willner, L.; Pipich, V.; Grillo, I.; Lindner, P.; Colmenero, J.; Richter, D. *Macromolecules* **2011**, *44*, 6145−6154.
(42) Bäverbäck, P.; Oliveira, C. L. P.; Garamus, V. M.; Varga, I.; Claesson, P. M.; Pedersen, J. *Langmuir* **2009**, *25*, 7296−7303.
(43) Lifshitz, I. M.; Slyozov, V. V. *J. Phys. Chem. Solids* **1961**, *19*, 35−50.
(44) Lund, R.; Willner, L.; Stellbrink, J.; Lindner, P.; Richter, D. *Phys. Rev. Lett.* **2010**, *104*, 049902.
(45) Choi, S.-H.; Bates, F. S.; Lodge, T. P. *Macromolecules* **2011**, *44*, 3594−3604.
(46) Aniansson, E.; Wall, S. N.; Almgren, M.; Hoffmann, H.; Kielmann, I.; Ulbricht, W.; Zana, R.; Lang, J.; Tondre, C. *J. Phys. Chem.* **1976**, *80*, 905−922.
(47) Meli, L.; Santiago, J. M.; Lodge, T. P. *Macromolecules* **2010**, *43*, 2018−2027.
(48) Dormidontova, E. E. *Macromolecules* **1999**, *32*, 7630−7644.
(49) Loverde, S. M.; Ortiz, V.; Kamien, R. D.; Klein, M. L.; Discher, D. E. *Soft Matter* **2010**, *6*, 1419.
(50) Fernyhough, C.; Ryan, A. J.; Battaglia, G. *Soft Matter* **2009**, *5*, 1674.
(51) Lund, R.; Willner, L.; Stellbrink, J.; Radulescu, A.; Richter, D. *Macromolecules* **2004**, *37*, 9984−9993.
(52) Sakya, P.; Seddon, J. M.; Templer, R. H.; Mirkin, R. J.; Tiddy, G. *Langmuir* **1997**, *13*, 3706−3714.
(53) Allgaier, J.; Poppe, A.; Willner, L.; Richter, D. *Macromolecules* **1997**, *30*, 1582−1586.
(54) Lindner, P. *Neutrons, X-Ray and Light. Scattering Methods Applied to Soft Condensed Matter*; Zemb, Th., Ed.; Elsevier: Amsterdam, 2002.